Investigation of the optical properties of InGaAsN/GaAs/GaAsP multiple-quantum-well laser with 8-band and 10-band $k\cdot p$ model

S. T. Ng, W. J. Fan, S. F. Yoon, and S. Z. Wang
School of Electrical and Electronic Engineering, Nanyang Technological University, Singapore 639798, Singapore

Yi Qu, C. Y. Liu, S. G. Ma, and Shu Yuan
School of Materials Engineering, Nanyang Technological University, Singapore 639798, Singapore

(Received 3 March 2004; accepted 20 July 2004)

We have used both 10-band and 8-band $k\cdot p$ Hamiltonian to investigate the maximum TE-mode optical gain for the triple quantum wells with $In_{0.35}Ga_{0.65}As_{0.985}N_{0.015}$ as the active layers and barriers comprised of two unstrained GaAs layers and one tensile-strained $GaAs_{0.82}P_{0.18}$ layer. The results were compared to a similar structure without the GaAsP layer and were discovered that the presence of the GaAsP barrier reduced the carrier density at threshold condition. However, the characteristics of the optical gain versus radiative current density for both structures are very similar. We also found the conduction band energy dispersion curves calculated by the 8-band model are flatter than the 10-band model due to the larger InGaAsN effective mass used. The transparent carrier density of the 10-band model is smaller than that of the 8-band model. The radiative recombination coefficient B calculated by the two models varies from 3.5×10^{-11} cm^3/s for the 8-band model to 8.0×10^{-11} cm^3/s for the 10-band model. Using $J_{tot}=n_w ql(AN+BN^2+CN^3)$, the calculated J_{th} of 558 A/cm^2 agrees very well with the experimentally observed threshold current density of a 10×1600 μm^2 broad-area laser. © *2004 American Institute of Physics*.
[DOI: 10.1063/1.1792804]

Over the past few years, the InGaAsN-based quantum wells (QWs) have received great attention. While the promising potential of this material to replace InGaAsP/InP QWs as the conventional laser source in telecommunication was initially hindered by the high threshold current observed in early grown samples, the recent effort to improve the threshold current by adding other III-V compounds into the barrier has proved to be a more challenging task. Thus far, Tansu *et al.* has been very successful in reducing the threshold current density J_{th} to 390 A/cm^2 using the direct barriers of GaAsP.[1] However, there is still no attempt of using it in a symmetrically structured InGaAsN/GaAs/GaAsP multiple quantum wells (MQW). In this paper, we used such structure to investigate the possibility of achieving low threshold current density and investigate the difference between the optical properties calculated by both 8-band and 10-band $k\cdot p$ models.

Instead of a single GaAs layer as the barrier, our structure used two unstrained GaAs layers and one GaAsP layer to form a combined barrier as shown in Fig. 1. This structure is believed to have a higher confinement potential than the single GaAs barrier due to the higher band-gap energy of GaAsP and is supposed to reduce the carrier leakage from the quantum well. The width of the active layers is 64 Å and the barrier width is 220 Å in total ($d_1=70$ Å, $d_2=80$ Å). A sample with such structure was grown by metal organic chemical vapor deposition. Subsequently, ridge laser diodes were fabricated using pulse anodic oxidation technique. In Fig. 2, we have plotted the measured output power versus injection current characteristic for the uncoated 10×1600 μm^2 broad-area laser operated in continuous-wave (CW) mode. As can be seen, the threshold injection current is about 89 mA, which corresponds to J_{th} of about 556 A/cm^2. The lasing wavelength is 1295 nm as measured by a spectrometer with Ge detector cooled down to −20 °C. The sample has been characterized extensively and reported elsewhere.[2] Here, we intend to address some aspect of the low threshold current density achieved by this structure using detailed calculation based on the $k\cdot p$ model.

We have previously investigated the optical gain of InGaAsN/GaAsN QWs by using a 6×6 $k\cdot p$ model.[3] To accurately simulate the energy dispersion curves of InGaAsN material, a 10-band $k\cdot p$ model,[4] which incorporates the band-anticrossing (BAC) (Ref. 5) model into the 8-band $k\cdot p$ model,[6] was developed by Choulis *et al.* Recently, the BAC model has been employed to explain the modification to band-gap energy,[7] effective mass,[8] and pressure-induced shifting of conduction band edge[5] when nitrogen atoms are

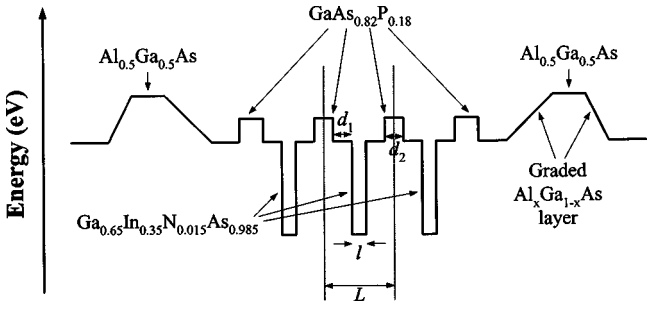

FIG. 1. Schematic band diagram for the $In_{0.35}Ga_{0.65}As_{0.985}N_{0.015}$ multiple quantum wells with barrier formed by tensile-strained $GaAs_{0.82}P_{0.18}$ and unstrained GaAs layers. d_1 and d_2 are the thickness of the GaAs and GaAsP barriers, respectively. l is the thickness of the compressive strained active layer.

added into $In_xGa_{1-x}As$ to form $In_xGa_{1-x}As_{1-y}N_y$ alloys. The interaction of localized N-induced resonant states with the extended states of the $In_xGa_{1-x}As$ conduction band has been cited as the main reason to cause the significant lowering of conduction band edge in III-N-V semiconductor compounds.[5] However, unlike the 10-band $k\cdot p$ model, the band-gap lowering and enhancement of the electron effective mass of InGaAsN (Ref. 9) must be specified explicitly as input to the 8-band $k\cdot p$ Hamiltonian. The Hamiltonian in Ref. 6 is modified to take into consideration the additional barrier potential and tensile strain in the GaAsP barrier. The strained conduction band offset Q_C for the $In_xGa_{1-x}As_{1-y}N_y/GaAs$ quantum well was determined from that of $In_xGa_{1-x}As/GaAs$ of same indium composition with the assumption that the unstrained valence band edge of the $In_xGa_{1-x}As/GaAs$ and $In_xGa_{1-x}As_{1-y}N_y/GaAs$ are the same. The Q_C for $GaAs_{1-x}P_x/GaAs$ was interpolated from the experimental values reported by Zhang *et al.*[10] All the other band parameters were collected from the compilation by Vurgaftman *et al.*[11]

The energy dispersion curves for conduction and valence subbands in the direction of [100] and [110] are shown in Fig. 3. As can be observed, the conduction band-energy dispersion curves of the 8-band model are flatter than those of the 10-band model due to the higher electron effective mass of $0.0987m_0$ used in the calculation.[9] Also in good agreement with the assumption of BAC, we observe only a small difference between the valence band energy dispersion curves calculated by both models. The calculated transition wavelength is 1297 nm (956 meV) for the 8-band model and 1243 nm (997 meV) for the 10-band model. While the heavier effective mass in the 8-band model proved to be a better fit for the experimentally observed lasing wavelength at 1295 nm; however, the separation between the first two electron energy levels are greatly reduced as compared to those computed by the 10-band model. The net effect is a greater density of states near the band edge of the conduction that must be filled by more carriers to achieve lasing threshold. We expect a better agreement between the predicted emission wavelength by the 10-band model and the experimental value if the many-body effects are being considered in the optical gain calculation. The typical shift caused by band-gap renormalization in $In_xGa_{1-x}As/GaAs$ QW has been

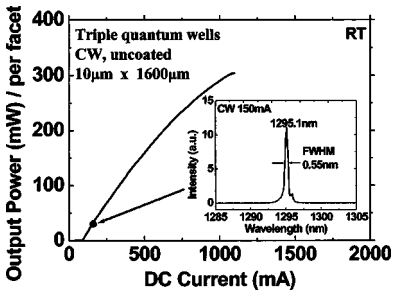

FIG. 2. CW light output power versus injection current measured at room temperature (RT) for a $10\times1600\ \mu m^2$ ridge waveguide $In_{0.35}Ga_{0.65}As_{0.985}N_{0.015}$ triple quantum wells. The inset shows the lasing spectrum of the MQW at an injection current of 150 mA.

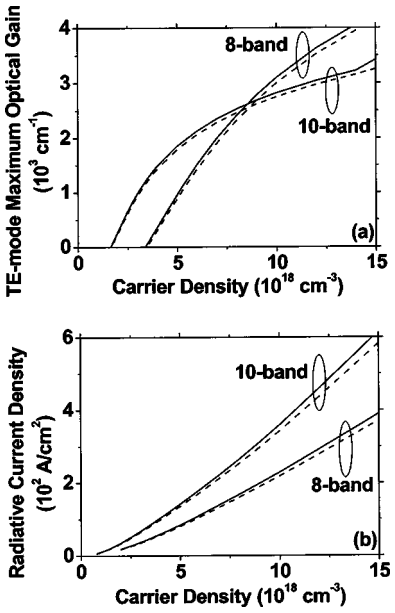

FIG. 4. (a) Maximum optical gain of the TE-mode as a function of carrier density. (b) Radiative current density as a function of carrier density. Solid lines are for structure *A*, dashed lines are for structure *B*.

shown to be around 40 to 50 meV,[12] which is just the value that is required to increase the calculated transition wavelength to 1.30 μm.

We have also plotted the maximum TE-mode optical gain obtained at different carrier density for both 10-band and 8-band models in Fig. 4(a) for both structure with or without GaAsP barriers. For simplicity, we will refer to the structure with GaAs/GaAsP/GaAs barrier as structure *A* and the other as structure *B*. The transparency carrier density N_{tr} obtained by the 10-band is much lower than the value predicted by the 8-band model, since N_{tr} is directly related to

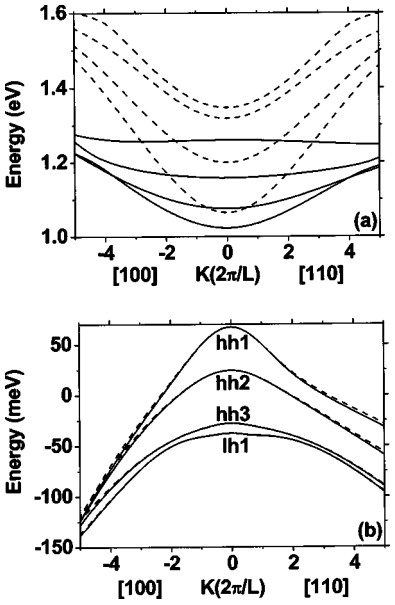

FIG. 3. The in-plane energy dispersion curves of the $In_{0.35}Ga_{0.65}As_{0.985}N_{0.015}$ quantum wells with $GaAs/GaAs_{0.82}P_{0.18}/GaAs$. (a) and (b) are the conduction and valence subbands, respectively. Solid line is the result calculated using 8-band $k\cdot p$ model, dashed line is that of the 10-band model.

the curvature of the energy dispersion of the conduction band as observed in Fig. 3. However, it is interesting to note that when compared to the GaAs barrier, the structure with GaAsP in the barrier actually delivers higher TE-mode optical gain at given carrier density. This is related to the increase in the confinement potential which not only increases the separation between the electron energy levels but also the separation between the quasi–Fermi-energy levels in the conduction and valence bands at fixed carrier density. Moreover, as observed in Fig. 4(b), the radiative current density J_{rad} for structure *A* with combined-barrier is slightly higher than the quantum wells with GaAs barriers alone. The increase in the barrier potential by the GaAsP layer has very little effect on the ground state energy but has elevated the higher excited states as can be observed from the difference between J_{rad} for structure *A* and *B*, which increased progressively with higher carrier density. The higher maximum optical gain calculated by the 8-band model at larger carrier density is attributed to the larger ratio of the InGaAsN electron effective mass over the heavy hole effective mass. From our calculations, we expect that structure *A* achieves the threshold condition with less N_{th}, and lower total current density if the Auger and monomolecular recombination coefficients remain unchanged for structure *A* and *B*.

With our calculated confinement factor of 9.1% for structure *A* and 9.45% for structure *B* and the experimental determined internal loss α_i of 12 cm^{-1},[2] we are able to compute the N_{th} and J_{rad} at threshold condition. By assuming uniform charge injection across the triple quantum wells, we determined that the radiative recombination coefficient *B* is 8.0×10^{-11} cm^3/s (10 band) and 3.5×10^{-11} cm^3/s (8 band) for structure *A*, and 7.7×10^{-11} cm^3/s (10 band) and 3.3×10^{-11} cm^3/s (8 band) for structure *B*. As can be seen the radiative recombination coefficient calculated by 10-band model is closer to the 9.5×10^{-11} cm^3/s reported by Fehse *et al.*[13] While *B* calculated by the 8-band model is almost half as small.

We are also interested to estimate the total threshold current density using $J_{tot}=n_w ql(AN+BN^2+CN^3)$, where n_w is the well number, *q* is the electron charge, and *l* is the width of the active layer. *A*, *B*, and *C* are the coefficients characterizing monomolecular, radiative, and Auger recombination, respectively. *N* is the carrier density in the QWs. By using $A=2.95\times10^8$ $1/s$ and $C=4\times10^{-29}$ cm^6/s from Ref. 13 and our calculated $B=8.0\times10^{-11}$ cm^3/s and $N_{th}=2.45\times10^{18}$ cm^{-3}, the calculated $J_{th}=557.7$ A/cm^2 agrees very well with the experimental value. From the above calculation, we would like to attribute the reduction in monomolecular recombination coefficient to the better crystal quality and the improved postgrowth preparation of our sample. However, the exact reduction in monomolecular recombination relies on the crystal quality and process, and is beyond the scope of this discussion.

In conclusion, we have calculated the optical properties of the InGaAsN quantum well with both GaAs barrier and GaAs/GaAsP/GaAs barrier and found that the latter structure resulted in smaller threshold carrier density. Moreover, *B* calculated by the 10-band $k\cdot p$ model is almost double that calculated by 8-band $k\cdot p$ model. We have also observed that the transparency carrier density N_{tr} calculated by 10-band model is generally smaller than that computed by the 8-band model due to the larger electron effective mass of InGaAsN used in the 8-band model which must be specified explicitly.

[1] N. Tansu, J.-Y. Yeh, and L. J. Mawst, Appl. Phys. Lett. **83**, 2112 (2003).
[2] Y. Qu, C. Y. Liu, S. G. Ma, and S. Yuan, IEEE J. Quantum Electron. (in press).
[3] W. J. Fan, S. T. Ng, S. F. Yoon, M. F. Li, and T. C. Chong, J. Appl. Phys. **93**, 5836 (2003).
[4] S. A. Choulis, T. J. C. Hosea, S. Tomic, M. Kamal-Saadi, A. R. Adams, E. P. O'Reilly, B. A. Weinstein, and P. J. Klar, Phys. Rev. B **66**, 165321 (2002).
[5] W. Shan, W. Walukiewicz, J. W. Ager III, E. E. Haller, J. F. Geisz, D. J. Friedman, J. M. Olson, and S. R. Kurtz, Phys. Rev. Lett. **82**, 1221 (1999).
[6] S. Ridene, K. Boujdaria, H. Bouchriha, and G. Fishman, Phys. Rev. B **64**, 085329 (2001).
[7] J.-Y. Duboz, J. A. Gupta, Z. R. Wasilewski, J. Ramsey, R. L. Williams, G. C. Aers, B. J. Riel, and G. I. Sproule, Phys. Rev. B **66**, 085313 (2002).
[8] J. B. Heroux, X. Yang, and W. I. Wang, J. Appl. Phys. **92**, 4361 (2002).
[9] W. W. Chow, E. D. Jones, N. A. Modine, A. A. Allerman, and S. R. Kurtz, Appl. Phys. Lett. **75**, 2891 (1999).
[10] X. Zhang, K. Onabe, Y. Nitta, B. Zhang, S. Fukatsu, Y. Shiraki, and R. Ito, J. Appl. Phys. **30**, L1631 (1991).
[11] I. Vurgaftman, J. R. Meyer, and L. R. Ram-Mohan, J. Appl. Phys. **89**, 5815 (2001).
[12] C.-F. Hsu, P. S. Zory, C.-H. Wu, and M. A. Emanuel, IEEE J. Sel. Top. Quantum Electron. **3**, 58 (1997).
[13] R. Fehse, S. Tomic, A. R. Adams, S. J. Sweeney, E. P. O'Reilly, A. Andreev, and H. Riechert, IEEE J. Sel. Top. Quantum Electron. **8**, 801 (2002).